AJNR

Posterior Fontanelle Sonography: An Acoustic Window into the Neonatal Brain

Flavia Correa, Goya Enríquez, José Rosselló, Javier Lucaya, Joaquim Piqueras, Celestino Aso, Elida Vázquez, Arantxa Ortega and Alfredo Gallart

This information is current as of April 16, 2024.

Posterior Fontanelle Sonography: An Acoustic Window into the Neonatal Brain

Flavia Correa, Goya Enríquez, José Rosselló, Javier Lucaya, Joaquim Piqueras, Celestino Aso, Elida Vázquez, Arantxa Ortega, and Alfredo Gallart

BACKGROUND AND PURPOSE: Sonographic brain studies are classically performed through the anterior fontanelle, but visualization of posterior supratentorial and infratentorial structures is poor with this approach. Posterior fontanelle sonography is recommended for better assessment of these structures. Our purpose was 1) to determine whether sonography of the brain through the posterior fontanelle (PF) improves visualization of brain lesions when added to the routine anterior fontanelle (AF) approach and 2) to describe standardized PF coronal and sagittal sections.

METHODS: In this prospective study (conducted from February 1999 to January 2001), PF sonography was added to AF sonography in 165 consecutive premature neonates with a birth weight of <2000 g. Sonograms were recorded in digital format for re-evaluation at the end of the study. Lesions were grouped as congenital, infectious, hemorrhagic, or hypoxic-ischemic. The χ^2 test for paired data and the κ coefficient were used to compare diagnoses with AF alone and diagnoses with AF plus PF.

RESULTS: PF sonography was performed in 164 of 165 patients: Results were normal in 86 and abnormal in 78. The single posterior fossa malformation detected in this series was best delineated with the PF approach. PF sonography increased the diagnostic rate of grade II hemorrhage by 32%. Cerebellar hemorrhage (two patients) and cerebellar abscesses (one patient) were diagnosed by using the PF approach. PF sonography did not contribute to the diagnosis of periventricular leukomalacia.

CONCLUSION: Study of the neonatal brain with the addition of PF sonography afforded greater accuracy in detecting intraventricular hemorrhage compared with AF sonography alone, especially when the ventricle was not dilated. The PF approach better defines posterior fossa malformations.

Sonography is the most widely used technique for imaging the neonatal brain owing to its low cost, accessibility, and safety. It has proven diagnostic value in detecting the most common brain lesions in premature neonates; such lesions include those due to intraventricular hemorrhage and white matter disease (1). Nevertheless, the accuracy of sonography of the brain is limited. Autopsy findings reveal that sonography causes underdiagnosis of intraventricular hemorrhage in 8–34% of cases (2–4). Sonographic studies of the brain are classically performed through the

anterior fontanelle (AF), but visualization of posterior supratentorial and infratentorial structures is poor with this approach. The mastoid fontanelle, also known as the posterolateral fontanelle, is located at the junction of the temporal, parietal, and occipital bones. The posterior fontanelle (PF) situated at the junction of the lambdoid and sagittal sutures should also be used for more complete study of the brain (Fig 1). This work focused on sonography via the PF, which provides excellent visualization of occipital lobes, occipital horns, and choroid plexuses. Some have suggested that the use of this fontanelle improves the accuracy of sonography for detecting hemorrhage in these regions (5, 6). The assessment of congenital malformations of the infratentorial compartment (7) and hypoxic-ischemic lesions affecting the most posterior parieto-occipital regions has also been considered an indication for the PF approach (8).

The aim of this study was to determine whether cranial sonography through the PF increases the detection rate or improves visualization of congenital malformations, infectious diseases, hemorrhage, and hypoxic-ischemic lesions in studies of the neonatal
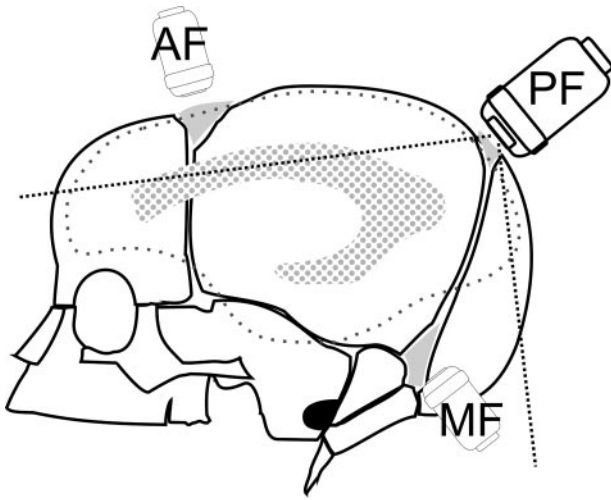
FIG 1.   Diagram shows the locations of the AF, PF, and mastoid fontanelle (MF).

brain. AF and PF findings were analyzed in 165 consecutive premature neonates.

Methods

From February 1999 to January 2001, PF sonography was added to routine AF sonography in all consecutive premature neonates with a birth weight of <2000 g. A total of 165 consecutive neonates were included: 87 boys and 78 girls, with gestational age range of 23–35 weeks (mean, 28.79 weeks) and a birth weight of 390–1990 g (mean, 1118 g). Sonograms were obtained by using two units (Aloka SSD-650; Aloka Co., Ltd, Tokyo, Japan, and 128 and Sequoia; Acuson, Mountain View, CA) equipped with 5–8-MHz sector transducers. The studies were performed by an experienced pediatric radiologist (G.E.) and a technician specialized in the study protocol. Written informed consent was obtained from the parents of all neonates.

Cranial sonography began through the AF and consisted of the acquisition of eight coronal sections followed by a sagittal midline sonogram and three sections on each side. The PF examination, which included coronal and sagittal views, was then performed with the neonate in the supine position with his or her head turned to one side for easier access to the fontanelle. To facilitate movement of the transducer, the imager could raise the patient's head slightly by using the nonimaging hand or a folded towel. The transducer was placed over the fontanelle and tilted slightly to obtain coronal views of the lateral ventricular trigones and occipital lobes, occipital horns, tentorium, and cerebellum (Fig 2). Sagittal views start at the midline following the sagittal suture. Structures visualized included the cerebellar vermis, fourth ventricle, cisterna magna, supracerebellar and quadrigeminal cisterns, pons, and medulla. The transducer was then rocked to obtain two parasagittal sections on each side of the midline to show the thalamus, choroid plexus, and entire occipital horn (Fig 3). PF sonography added a maximum of 5 minutes to the total examination time.

Patients underwent cranial sonography within the first 4 days of life, during the 2nd week, and at 1 month of age. In patients with lesions, sonography was repeated as necessary to monitor abnormal features. When studies through either AFs or PFs showed no abnormalities, the results were considered normal. However, if either or both of the approaches revealed an abnormal image the first time, the study was used for statistical analysis. The remaining follow-up studies were used to monitor possible complications (eg, hydrocephaly) or to reaffirm the initial diagnosis of the anomaly (eg, change in echogenicity of the clot, and cavitation in periventricular leukomalacia).

Images were recorded in digital format by using a PACS (Inturis; Philips, Best, the Netherlands). After all 165 patients had been studied, the images were reviewed by two authors (F.C., G.E.) simultaneously. They were blinded to clinical, pathologic, and other radiologic reports.

AF images were always read before PF images for each patient. The two readers determined by consensus what additional features were detected with the PF and scored the images for quality of visualization as follows: not seen (−), suspected (+), identifiable (++), and excellently visualized (+++).

Because the criteria for diagnosing intraventricular and choroid plexus hemorrhage by using the PF approach are not well established, we used the following sonographic features for this purpose. Intraventricular hemorrhage was defined by the presence of echogenic material in the ventricle, extending beyond the calcarine fissure (a deep sulcus situated on the medial surface of the occipital cortex) or by visualization of intraventricular layering (fluid-fluid level, CSF, and blood). Choroid plexus hemorrhage was characterized by alteration of the choroid contour or a heterogeneous appearance (hypoechoic areas).

Following the Papile classification (9), subependymal and intraventricular hemorrhages were classified into three groups according to severity: Grade I hemorrhage was confined to the germinal matrix, grade II was intraventricular hemorrhage with slight or no dilatation of the lateral ventricle, and grade III was intraventricular hemorrhage with ventricular dilatation. For statistical analyses, hemorrhage confined to the choroid plexus was classified as grade II. Echogenic periventricular lesions associated with substantial ventricular hemorrhage (formerly Papile grade IV) were referred to as hemorrhagic venous infarcts (10). Cerebellar hemorrhage was diagnosed when hyperechoic areas were present in the cerebellum; these were hypoechoic on follow-up studies.

The χ^2 test for paired data were used to determine whether the percentage of diagnoses was the same with AF sonography alone as with AF-plus-PF sonography. Significance was set at a P value <.05. Concordance between the two measurements was determined with the κ coefficient. CIs were calculated at 95%. Calculations were carried out by using the Statistical Package for Social Sciences software (SPSS; Chicago, IL). Statistical comparison of AF and PF findings was performed by using the first studies that showed abnormal findings or suspected abnormal findings for each patient.

Autopsy results were available for 10 (50%) of the 20 neonates who died. Intervals between the last sonographic study and death were as follows: same day (one case), following day (five cases), 2 days (two cases), 5 days (one case) and 7 days (one case). A pediatric pathologist removed the brain, fixed it in 10% formaldehyde buffered to pH = 7, and stabilized it with methanol for 2 weeks. After reviewing the clinical history and sonographic findings, the pathologist visually analyzed the specimen. The cerebellum and brain stem were dissected, and the rest of the brain was sectioned, following the eight coronal sonograms beginning with the frontal lobes. Coronal sections of the cerebellum and brain stem were also obtained. The brain stem and cerebellum were sectioned together in very premature neonates. Finally, sonographic and autopsy findings were compared.

Results

One of the 165 neonates could not be examined with the PF approach, because the neonate was clinically unstable and could not be moved. For the remaining 164 patients, sonographic results were normal in 86 (52.5%) and abnormal in 78 (47.5%). For analysis, the lesions were attributed to congenital malformations, infectious diseases, hemorrhagic lesions, and hypoxia-ischemia.

Fig 2. Normal coronal sections of the PF (superior to inferior). *CA* indicates calcar avis; *Ch*, choroid plexus; *CH*, cerebellar hemispheres; *LV*, lateral ventricle trigone; *OH*, occipital horn; *OL*, occipital lobe; *SA*, subarachnoid space; and *T*, tentorium.

A–C, Images in a neonate at 30 weeks' gestational age.

A, The most superior coronal view.

B, The middle coronal view.

C, The inferior view.

D, Same section as in *C* in a neonate at 25 weeks' gestational age shows a more rounded configuration of occipital horns and a wide (up to 15 mm) subarachnoid space with internal echogenic dots corresponding to vessels.
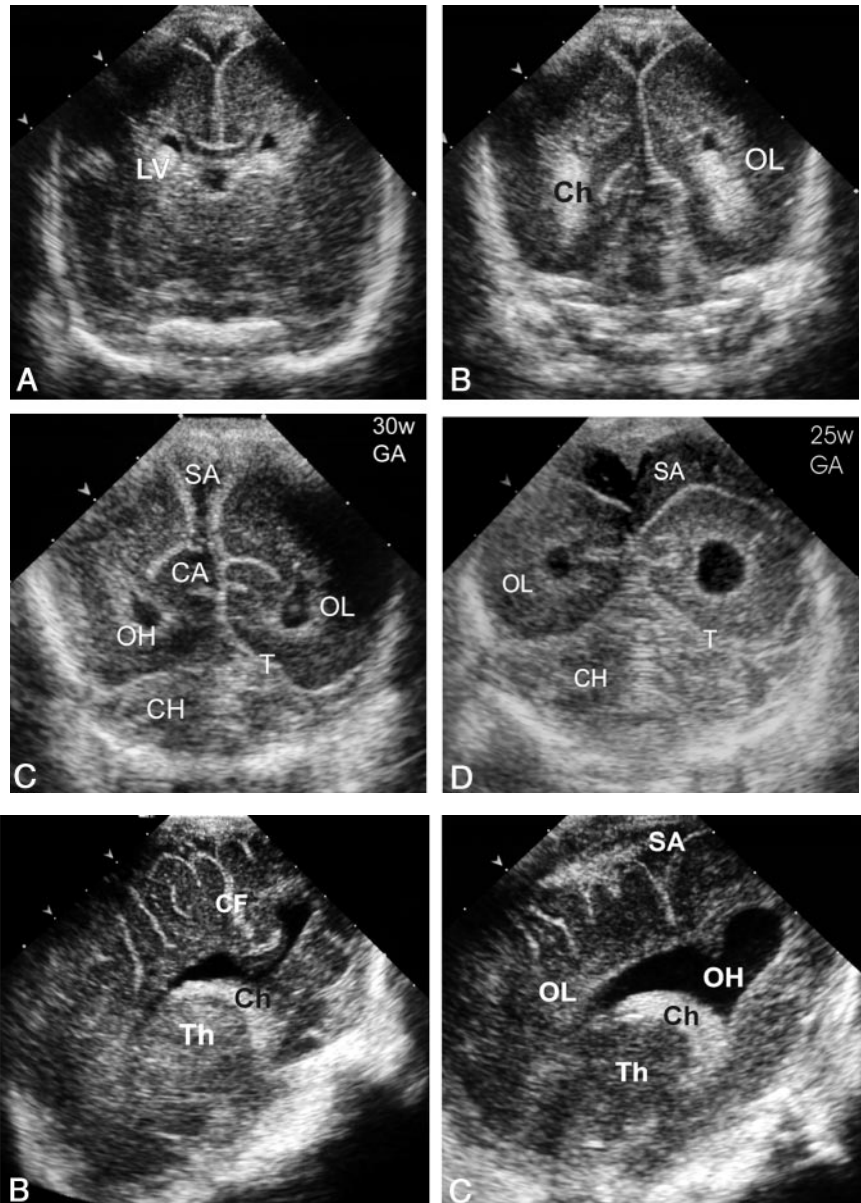

Fig 3. Normal sections of the PF. *CF* indicates calcarine fissure; *Ch*, choroid plexus; *FM*, foramen magnum; *M*, medulla; *OH*, occipital horn; *OL*, occipital lobe; *OS*, occipital squama; *PO*, parieto-occipital fissure; *QC*; quadrigeminal cistern; *S*, aqueduct of Sylvius; *SA*, subarachnoid space; *SC*, supracerebellar cistern; *Th*, thalamus; *V*, vermis; and *4V*, fourth ventricle.

A, Midsagittal view.

B, Parasagittal view.

C, More lateral parasagittal view.

Congenital Malformations and Infectious Disease

Only one malformation, a megacisterna magna, was found in our series. The presence of a cystic lesion in the posterior fossa was seen with AF sonography; however, the PF view showed a normal vermis with the lesion surrounding it, thereby establishing the diagnosis of megacisterna magna (Fig 4). Two neonates had lesions resulting from infectious disease: One was due to *Candida albicans* and the other to *Staphylococcus aureus*. Both were confirmed by means of microbiologic testing and MR imaging. In the first case, a premature neonate had been treated with prolonged antibiotic therapy, and PF sonography improved visualization of the microabscesses in the frontal and parietal lobes and ruled out

cerebellar involvement (Fig 5). The second patient had been examined soon after birth, and sonographic findings were normal. However, at the age of 45 days, that patient was brought to the emergency room because of lethargy and a bulging fontanelle. PF sonography depicted two abscesses in the left cerebellar hemisphere that were not seen with the AF approach. Sonographic findings concurred with MR imaging results (Fig 6).

Hemorrhagic Lesions

Thirty-three patients (20%) had grade I hemorrhage, which was seen through both fontanelles in three patients (95% CI: 3–24%), through only the AF
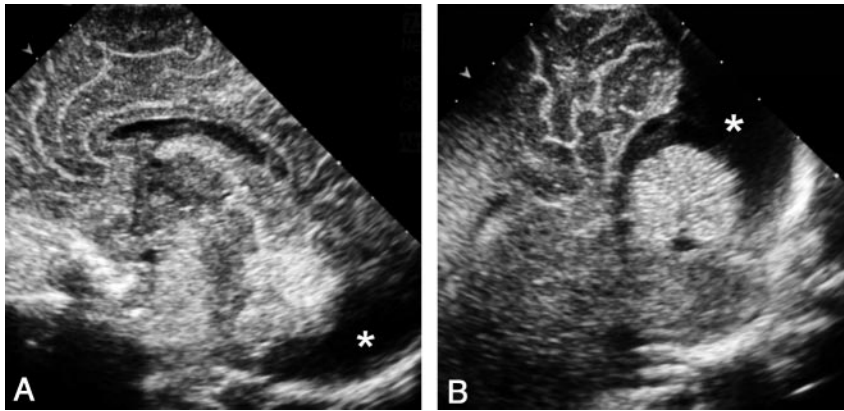
Fig 4. Sonograms obtained in a neonate with a presumptive diagnosis of posterior fossa malformation at prenatal sonography.

A, AF midline sagittal view shows a cystic image (*asterisk*) in the posterior fossa behind the cerebellum.

B, PF midline sagittal view clearly demonstrates that the lesion corresponds to a megacisterna magna, depicting the normal-sized cerebellum vermis and fourth ventricle. Note that the cystic lesion (*asterisk*) extends around the cerebellum without compressing it, as often occurs with arachnoid cysts.
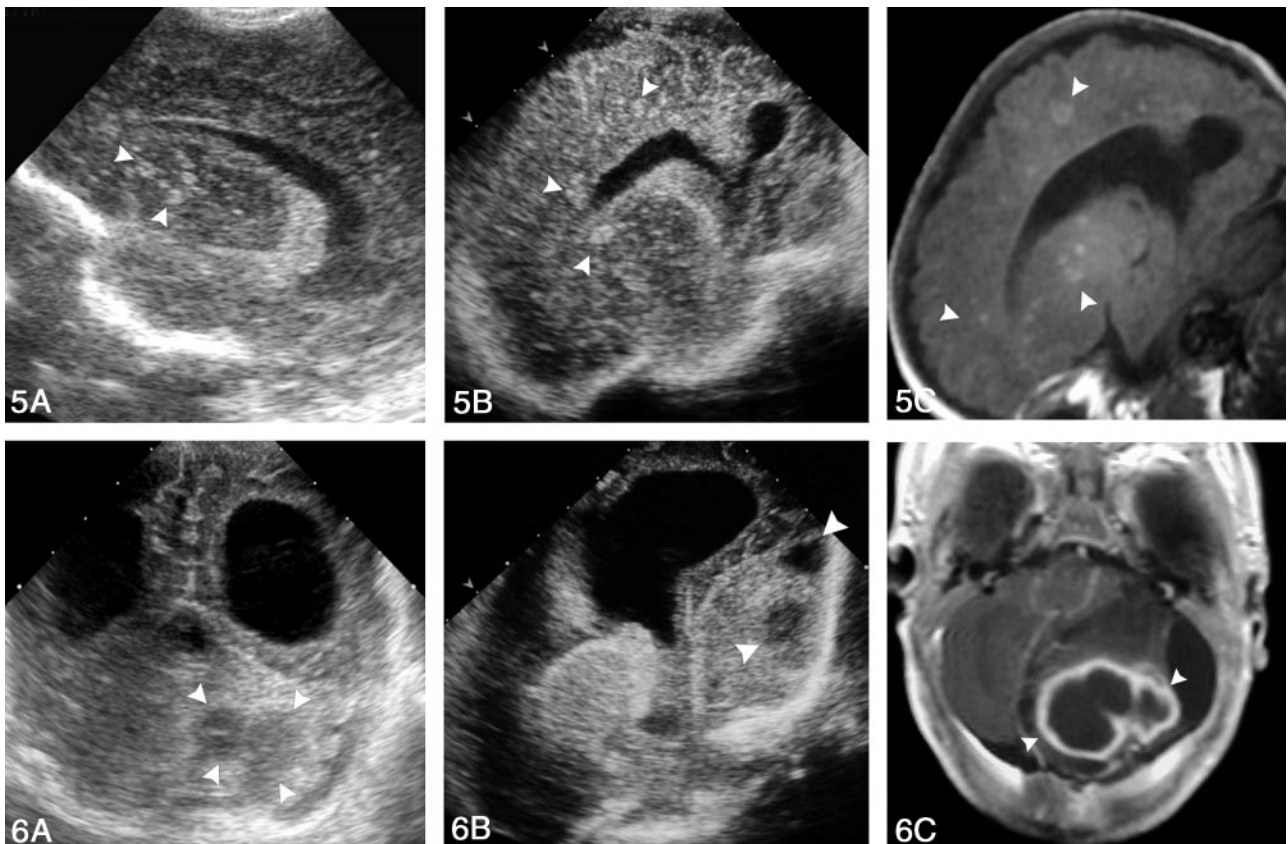

Fig 5. Images obtained in a premature neonate with systemic candidiasis treated with prolonged antibiotic therapy; disease was confirmed on the basis of blood culture findings.

A, AF right parasagittal sonogram demonstrates multiple, rounded, hyperechoic nodules—some with central umbilication—affecting the basal nuclei (*arrowheads*).

B, PF right parasagittal sonogram also shows multiple, rounded, hyperechoic lesions affecting the frontal and parietal lobes (*arrowheads*).

C, Parasagittal T1-weighted MR image confirms the sonographic findings. (The child survived, and the lesions [*arrowheads*] calcified.)

Fig 6. Images of cerebellar abscesses in a 45-day-old neonate presenting with AF bulging and lethargy. A culture of fine-needle aspiration material isolated *S aureus*.

A, PF coronal sonogram reveals bilateral occipital horn dilatation and enlarged left cerebellar hemisphere with two hypoechoic lesions (*arrowheads*).

B, PF left parasagittal sonogram shows lateral ventricle dilatation and the cerebellar abscesses (*arrowheads*).

C, Contrast-enhanced T2-weighted MR image confirms the sonographic findings (*arrowheads*).

in 29 (89%; 95% CI: 71–96%) and more clearly through the PF in one (3%; 95% CI: 1–15%) owing to its posterior location (Fig 7). Therefore, AF sonography was significantly better than PF sonography for the detection of grade I hemorrhage ($P = .001$).

Grade II hemorrhage was identified in 28 patients (17%). In 12 cases (43%; 95% CI: 27–61%), the diagnosis was established by findings from both approaches. In nine cases (32%; 95% CI: 18–51%), findings of AF study were considered normal, and
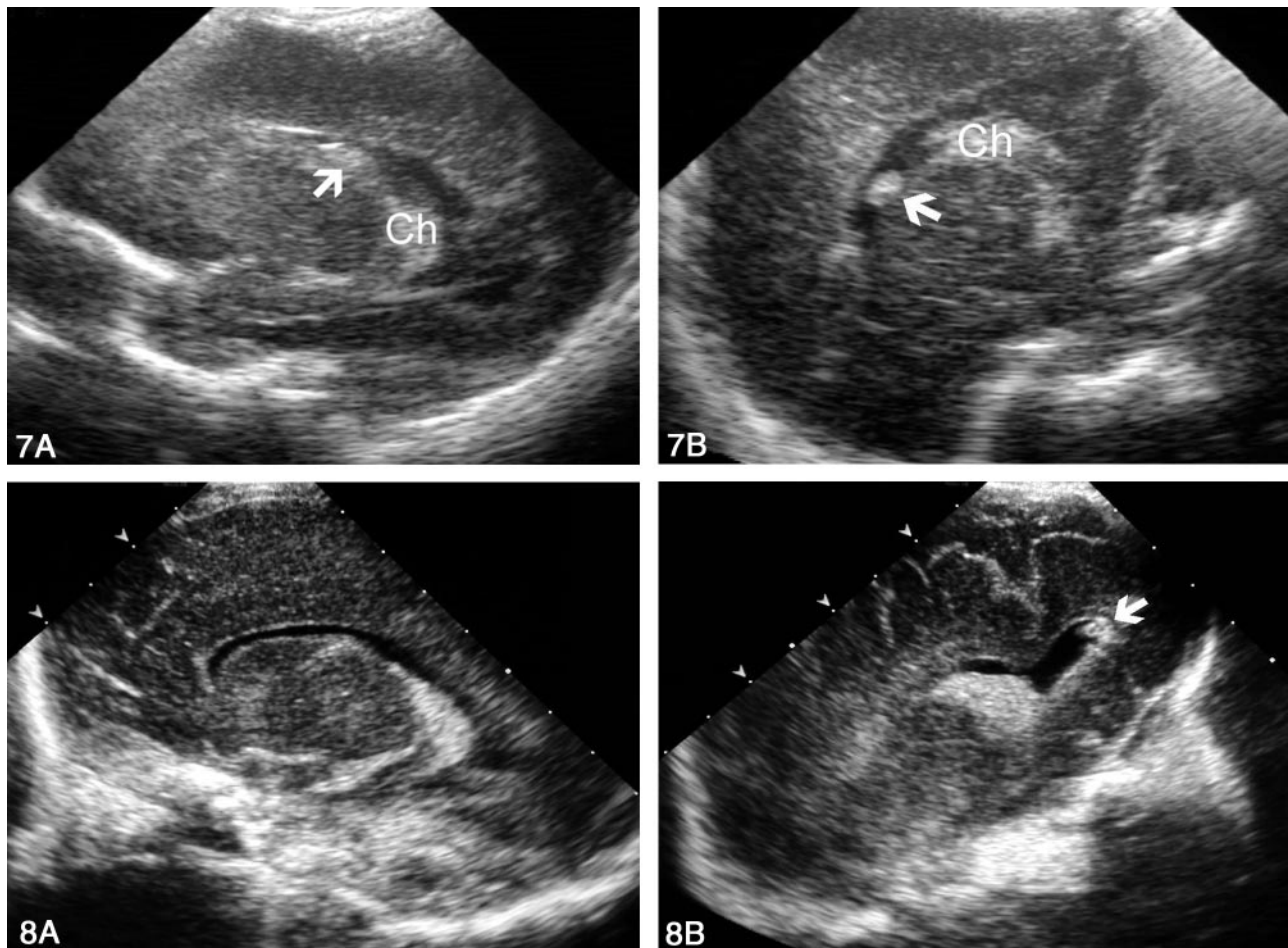
Fig 7.   Sonograms obtained in a premature neonate with grade I hemorrhage that was better delineated through the PF than through the AF.

A, AF left parasagittal view shows an equivocally echogenic image (*arrow*). The choroid plexus (*Ch*) is not well depicted.

B, PF left parasagittal view clearly depicts the echogenic lesion (*arrow*) independent of the choroids (*Ch*). On follow-up studies, the lesion disappeared.

Fig 8.   Sonograms obtained in a premature neonate with grade II hemorrhage.

A, AF left parasagittal view shows a normal-appearing left lateral ventricle.

B, PF left parasagittal view reveals a small clot in the posteriormost portion of the occipital horn (*arrow*).

intraventricular hemorrhage was diagnosed on the basis of an additional PF study (Fig 8). In seven cases (25%; 95% CI, 13–43%) AF findings were equivocal, as it was not possible to conclusively determine whether anomalous intraventricular content was present. In this group, PF sonography was required in two cases to clarify whether the content was anomalous (two cases, Figs 9 and 10) or if a false-positive finding was due to the calcar avis (five cases, Fig 11). No case was identified by using only the AF approach. Therefore, PF sonography significantly improved the diagnosis of Grade II hemorrhage ($P = .001$, Table).

Grade III hemorrhage was detected in 12 patients (7%). All grade III hemorrhages were identified with both approaches. No difference was observed in the number of cases detected with the addition of PF sonography.

Hemorrhagic venous infarction (formerly Papile grade IV) occurred in 15 patients (9%). Eight cases (53%; 95% CI: 30–75%) were detected with both approaches, and seven cases (47%; 95% CI: 25–70%) with the anterior approach alone. Sonography through

the PF did not improve diagnostic performance. AF sonography was statistically superior to the posterior approach for revealing the lesion ($P = .03$).

Unequivocal diagnoses of cerebellar hemorrhage were based on PF findings in two patients. In the first, the bilateral cerebellar hemorrhage was not associated with intraventricular hemorrhage. At AF sonography, a subtentorial echogenic area of doubtful cerebellar or extracerebellar origin was seen. The PF view clearly demonstrated bilateral cerebellar hemorrhage (Fig 12). In the second patient, massive intraventricular hemorrhage was accompanied by a left cerebellar hemorrhage. The former hindered visualization of the cerebellum on the AF view owing to slight shadowing; however, the left cerebellar hemorrhage was clearly seen on PF sonograms (Fig 13).

Hypoxic-Ischemic Lesions

Focal periventricular leukomalacia was diagnosed in 10 neonates. Comparison of the results obtained
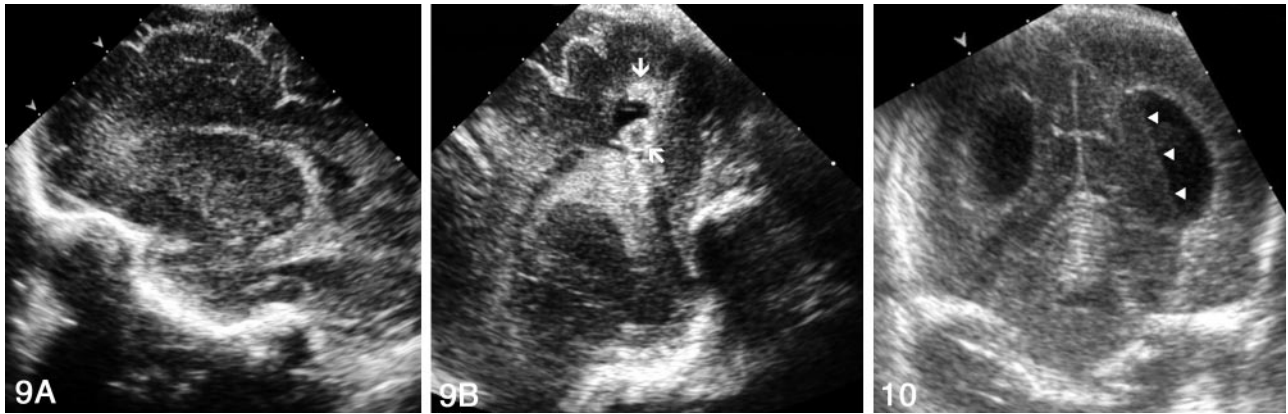
Fig 9. Sonograms obtained in a premature neonate with grade II intraventricular hemorrhage.
  A, AF right parasagittal view shows inconclusive appearance of the choroid plexus.
  B, PF right parasagittal view clearly depicts two clots in the occipital horn (*arrows*).

Fig 10. Sonogram of the occipital horn layering. Coronal PF view shows a fluid-fluid level (*arrowheads*) caused by blood and CSF in a slightly dilated left occipital horn.
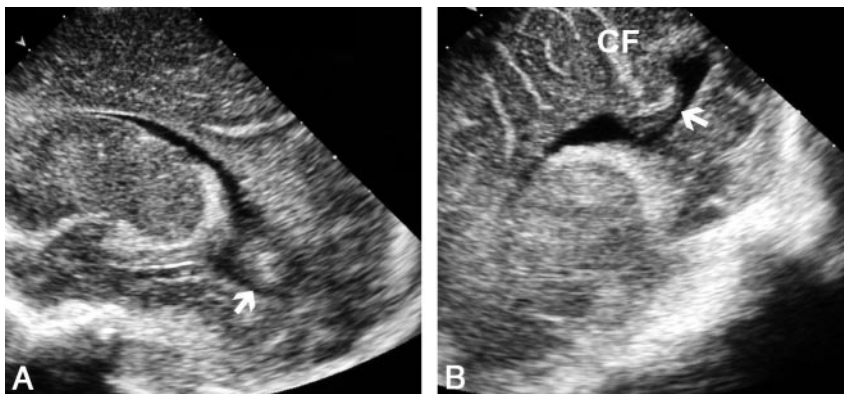

Fig 11. Sonograms of the calcar avis simulating intraventricular hemorrhage.
  A, AF parasagittal view shows a rounded masslike image mimicking an intraventricular clot within the occipital horn (*arrow*).
  B, PF parasagittal view demonstrates that the mass is the calcar avis (*arrow*). Note its continuity with the occipital white matter and the calcarine fissure (*CF*).

Statistical analysis of the diagnosis of hemorrhagic lesions with AF and PF sonography

Hemorrhage	Better Approach for Diagnosis	P Value, McNemar Test	Kappa Index (95% CI)
Grade I	AF	.001	0.165 (0.028, 0.301)
Grade II	PF	.001	0.517 (0.336, 0.698)
Grade III	AF and PF equal	>.05	0.889 (0.764, 1.013)
Hemorrhagic infarction	AF	.034	0.647 (0.421, 0.873)

with PF sonography; the AF view showed normal findings. Periventricular venous infarction was present in three cases. Sonographic diagnosis of cerebellar hemorrhage was confirmed in one patient. In two of the three patients in whom subarachnoid hemorrhage was found at autopsy, both AF and PF sonographic findings had been considered normal (Fig 15).

Discussion

The PF approach, which was formerly considered useful (7, 11, 12), has been virtually neglected. Now, it is used only as a window for studying the neonatal brain, thanks in part to the improvement in the design of transducers, which have been reduced in size (13). The purpose of PF sonography is to locate near-field structures far from the transducer through the AF. Brain structures that are particularly well depicted with the PF approach include the occipital lobes, the occipital horns, the choroid plexuses, and the basal cisterns.

Although routine study of the brain in premature neonates consists of AF sonography in coronal and sagittal views, we added PF sonography to evaluate for the presence of a prominent occipital horn, to clarify a suspicious appearance of choroid plexuses (size, contours, or echogenicity), to resolve doubts regarding ventricular content (calcar avis, clots, and

with the addition of PF sonography showed that the approach did not significantly contribute to establishing the diagnosis of this condition (*P* = .18) (Fig 14).

Comparison of Sonographic and Necropsy Findings

Necropsy studies of the brain were performed in 10 neonates. Autopsy and sonographic findings were normal in three patients. In the group with hemorrhages, autopsy findings confirmed the sonographic diagnosis of intraventricular hemorrhage in seven patients: one grade II and six grade III. In the grade II case, a clot in the left occipital horn was detected only
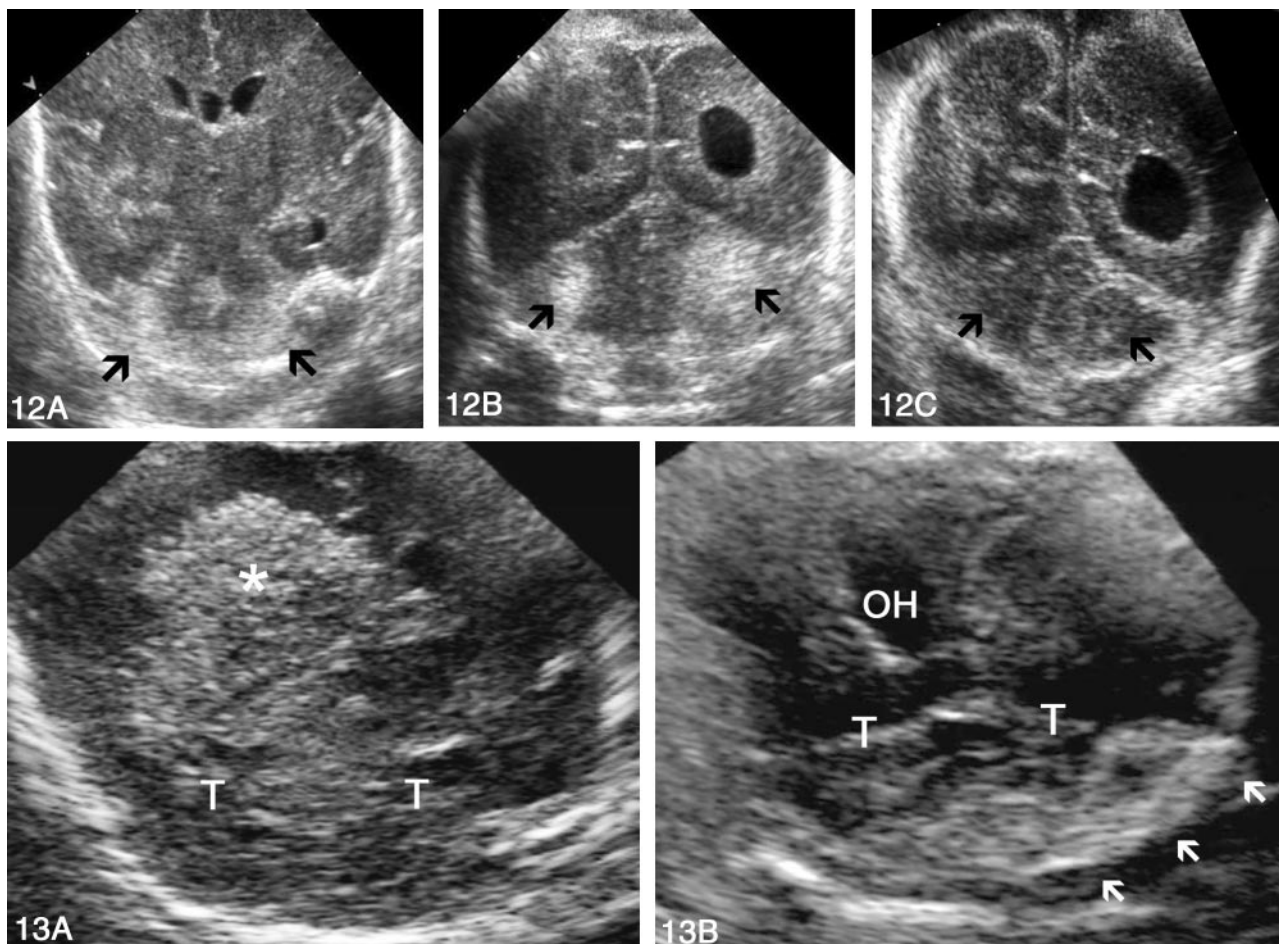
FIG 12. Sonograms of bilateral cerebellar hemorrhage obtained in a neonate without intraventricular hemorrhage at 30 weeks' gestational age.

A, AF coronal view shows the lateral ventricles to be normal. Echogenic areas in the subtentorial space (*arrows*) of indistinct cerebellar or extracerebellar origin are seen.

B, PF coronal view clearly reveals bilateral cerebellar hemorrhages (*arrows*).

C, PF coronal view obtained 1 week later shows that the hemorrhages have decreased in size and echogenicity (*arrows*).

FIG 13.   Sonograms obtained in a premature neonate with massive intraventricular and unilateral cerebellar hemorrhages. *T* indicates tentorium.

A, AF coronal view shows echogenic material occupying the right lateral ventricle (*asterisk*) that hinders correct visualization of the cerebellum owing to slight shadowing.

B, PF coronal view clearly depicts left echogenic cerebellar hemorrhage (*arrows*). *OH* indicates the occipital horn.

FIG 14. Sonograms of abnormal peritrigonal hyperechogenicity in a premature neonate with periventricular leukomalacia.

A, AF left parasagittal view depicts heterogeneous peritrigonal hyperechogenicity with areas of cavitation.

B, PF left parasagittal view. Coarse peritrigonal echogenicity and cavities are evident.
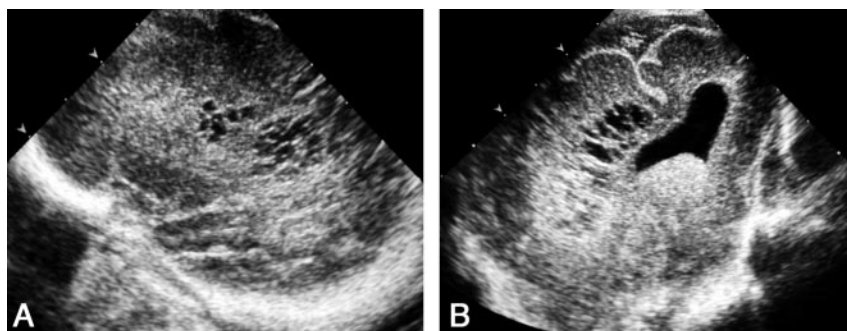
artifacts), and to assess marked lateral ventricle asymmetry; these situations account for approximately 90% of our cases. Coronal and sagittal views through the PF can be standardized in the same way as in AF study and add approximately 5 minutes to the examination.

The most important contribution of PF sonography in our study was the increased detection of grade II hemorrhage (32% more cases, 95% CI: 19–52%). This improved diagnostic rate was mainly attributable to the following factors: First, intraventricular clots migrate to the occipital horn, the most dependent
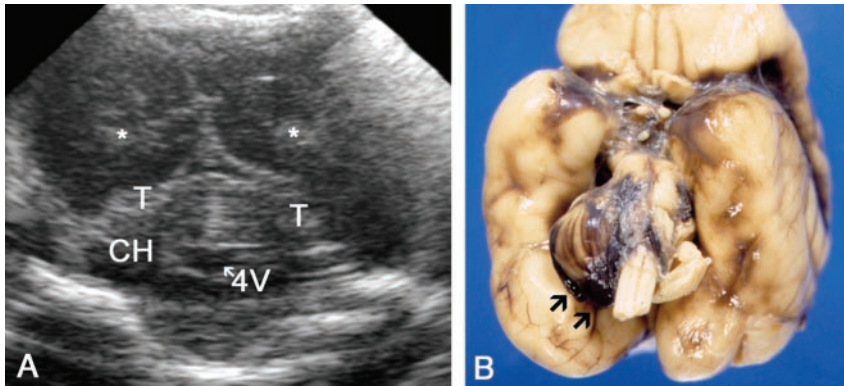
Fig 15. Sonogram and gross specimen obtained in a patient with discrepant findings at sonography and autopsy.

A, PF coronal sonogram shows echogenic material in the occipital horns (*asterisk*) corresponding to intraventricular hemorrhage. The cerebellum and basal subarachnoid space seem normal. *CH* indicates cerebellar hemispheres; *T*, tentorium; and *4V*, fourth ventricle.

B, Macroscopic view of the specimen 1 day later shows a hemorrhage surrounding the right cerebellar hemisphere.

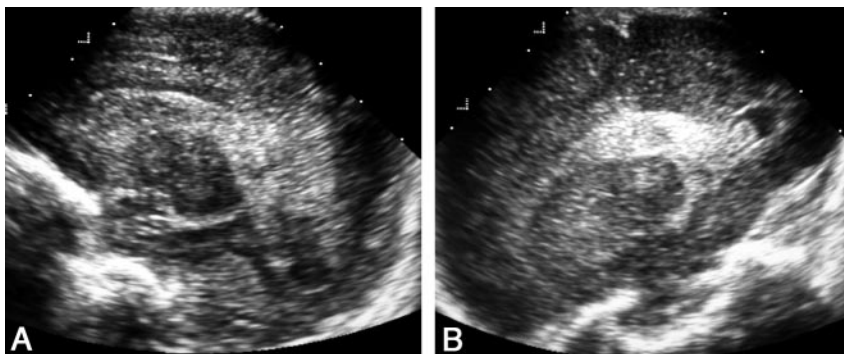Fig 16. Sonograms of a hemorrhage originating in the left choroid plexus.

A, AF left parasagittal view shows an inconclusive choroid appearance.

B, PF left parasagittal view depicts an enlarged choroid with heterogeneous echogenicity due to internal hemorrhage.

portion of the lateral ventricle, and are easily overlooked on AF views, particularly when the ventricle is normal in size or only slightly dilated (Fig 8). Second, intraventricular blood is usually more echogenic than CSF, but fresh liquefied blood and CSF may have similar echogenicity or differ slightly; therefore, the former may be mistaken for a reverberation artifact on AF sonograms. With the PF approach, the layers of CSF and fresh blood are seen as a fluid-fluid level owing to the angle of the sonographic echo on the ventricular wall (Fig 10). Finally, intraventricular hemorrhage in the premature neonate is classically thought to originate in the germinal matrix, but it can also start in the choroid plexus (13); delineation of this structure is optimal with PF views. The choroid plexus is highly echogenic and has a smooth, sharply defined contour. In the sagittal view, it assumes a semicircular form around the thalamus and thickens at the ventricular atrium to form the glomus (14). At PF sonography, choroid hemorrhage should be suspected when the plexus is increased in size, extending beyond the calcarine fissure, or when it shows heterogeneous echogenicity (Fig 16). The ability of the PF to depict grade II hemorrhage acquires importance in light of recent follow-up data showing that children with even low-grade hemorrhage may present with some degree of cognitive disability compared with their normal gestation- and age-matched peers (15). The fact that the PF approach is not generally used in brain studies of premature neonates may account for the high percentage of false-negative results in the diagnosis of intraventricular hemorrhage when sonographic studies of the AF alone are compared with autopsy findings (2, 4).

The PF view also clearly depicts the calcar avis, a structure that may produce misleading features on AF views, as in five of our patients. The calcar avis is a mound of occipital white matter protruding into the occipital horn and varies greatly in size from patient to patient and from side to side in the same patient (16). When sonography through the AF is performed, the calcar avis may be superimposed on the ventricle, simulating intraventricular hemorrhage. On posterior views, this anatomic structure is easily differentiated from intraventricular clot by noting its continuity with the occipital white matter and by identifying the calcarine fissure (Fig 11) (17).

Periventricular leukomalacia is the most common hypoxic-ischemic brain injury in the premature neonate and considered a major neurologic cause of spastic motor deficits. There are two well-recognized forms of periventricular leukomalacia: diffuse and focal. Diffuse periventricular leukomalacia is the most frequent, and its diagnosis is usually based on diffusion-weighted MR imaging results rather than sonographic findings (18). The focal form is characterized by necrotic lesions in the periventricular white matter, which can be recognized by use of sonography. Some authors have stated that the PF approach is useful for distinguishing normal peritrigonal blush from focal periventricular leukomalacia: The blush disappears in views through the PF, whereas lesions persist (8). In our experience, this is not a constant phenomenon, and we do not base the diagnosis on this fact. Instead, we consider bulbous or heterogeneous echogenicity in the periventricular area, sometimes with cavities in more advanced phases, a more useful sonographic criterion.

Neonates with meningitis are not routinely examined in our department, unless they fail to respond well to medical treatment or unless they present with complications. Therefore, only two neonates had lesions due to infectious disease in our series. PF sonography was particularly useful in both. One patient was a premature neonate receiving long-term antibiotic therapy. The diagnosis of candidiasis was suggested by the presence of generalized hyperechogenic lesions, some with central umbilication. PF sonography improved visualization of the microabscesses in the frontoparietal lobes. Involvement of basal nuclei was seen equally well with the two approaches. In the second patient, PF sonograms depicted two cerebellar abscesses due to *S aureus*; these were not seen with the AF approach. Complementary MR imaging confirmed the sonographic findings in both patients.

Because most of the neonates in our series were born very prematurely, additional imaging studies, such as CT and MR imaging, were performed only when they were considered absolutely necessary. Therefore, no criterion standard is available to establish the sensitivity and specificity of sonography in the diagnosis of intracranial lesions. We attempted to counterbalance this limitation by strictly defining the sonographic criteria for normal and abnormal findings, according to a series of straightforward features that can be readily standardized in clinical practice.

Conclusion

The PF approach played an important role in the diagnosis of intraventricular hemorrhage, both by confirming it and ruling it out. PF sonography also provided useful diagnostic information on congenital cystic malformations and infections in the posterior fossa. The addition of this approach to anterior sonography substantially increases the examiner's confidence in studying the neonatal brain.

Acknowledgments

References

1. Bulas DI, Vezina GL. **Preterm anoxic injury: radiologic evaluation.** *Radiol Clin North Am* 1999;37:1147–1161
2. Hope PL, Gould SJ, Howard S, Hamilton PA, Costello AM, Reynolds EO. **Precision of ultrasound diagnosis of pathologically verified lesions in the brains of very preterm infants.** *Dev Med Child Neurol* 1988;30:457–471
3. Mack LA, Wright K, Hirsch JH, et al. **Intracranial hemorrhage in premature infants: accuracy of sonographic evaluation.** *AJR Am J Roentgenol* 1981;137:245–250
4. Babcock DS, Bove KE, Han BK. **Intracranial hemorrhage in premature infants: sonographic-pathologic correlation.** *AJNR Am J Neuroradiol* 1982;3:309–317
5. Anderson N, Fulton J. **Sonography through the posterior fontanelle in diagnosing neonatal intraventricular hemorrhage.** *AJNR Am J Neuroradiol* 1991;12:368–370
6. Anderson N, Allan R, Darlow B, Malpas T. **Diagnosis of intraventricular hemorrhage in the newborn: value of sonography via the posterior fontanelle.** *AJR Am J Roentgenol* 1994;163:893–896
7. Maertens P. **Imaging through the posterior fontanelle.** *J Child Neurol* 1989;4:S62–S67
8. DiPietro MA, Brody BA, Teele RL. **Peritrigonal echogenic "blush" on cranial sonography: pathologic correlates.** *AJR Am J Neuroradiol* 1986;146:1067–1072
9. Papile LA, Burstein J, Burstein R, Koffler H. **Incidence and evolution of subependymal and intraventricular hemorrhage: a study of infants with birth weight less than 1500 gm.** *J Pediatr* 1978;92:529–534
10. Volpe JJ. **Intracranial hemorrhage: germinal matrix–intraventricular hemorrhage of the premature infant.** In: Volpe JJ, ed. *Neurology of the Newborn.* 3rd ed. Philadelphia: WB Saunders; 1995:403–463
11. Anderson NG, Hay R, Hutchings M, Whitehead M, Darlow B. **Posterior fontanelle cranial ultrasound: anatomic and sonographic correlation.** *Early Hum Dev* 1995;42:141–152
12. De Vries LS, Eken P, Beek E, Groenendaal F, Meiners LC. **The posterior fontanelle: a neglected acoustic window.** *Neuropediatrics* 1996;27:101–104
13. Di Salvo DN. **A new view of the neonatal brain: clinical utility of supplemental neurologic US imaging windows.** *RadioGraphics* 2001;21:943–955
14. Fiske CHE, Filly RA, Callen PW. **The normal choroid plexus: ultrasonographic appearance of the neonatal head.** *Radiology* 1981;141:467–471
15. Ment LR, Schneider KC, Ainley MA, Allan WC. **323 Adaptive mechanisms of developing brain: the neuroradiologic assessment of the preterm infant.** *Clin Perinatol* 2000;27:303–323
16. DiPietro MA, Brody BA, Teele RL. **The calcar avis: demonstration with cranial US.** *Radiology* 1985;156:363–364
17. Enriquez G, Correa F, Lucaya J, Piqueras J, Aso C, Ortega A. **Potential pitfalls in cranial sonography.** *Pediatr Radiol* 2003;33:110–117
18. Inder T, Huppi PS, Zientara GP, et al. **Early detection of periventricular leukomalacia by diffusion-weighted magnetic resonance imaging techniques.** *J Pediatr* 1999;134:631–634